

Glass Forming Ability and Mechanical Properties of $Zr_{57.52}Co_{21.24}Al_{9.24}Ag_{12}$ bulk metallic glass

Carlos Ernesto Borja Soto^{a,*}, Ignacio Alejandro Figueroa Vargas^b, Gabriel Ángel Lara Rodríguez^b,

Jorge Alejandro Verduzco Martínez^a

^a Instituto de Investigación en Metalurgia y Materiales, Universidad Michoacana de San Nicolás de Hidalgo- UMSNH, Fco. J. Mújica, S/N, Col. Felicitas del Río, C.P. 58030, Morelia, Mich., México

^b Instituto de Investigaciones en Materiales, Universidad Nacional Autónoma de México - UNAM, Circuito Exterior, S/N, Cd. Universitaria, C.P. 04510, México, D.F., México

Received: October 13, 2015; Revised: September 06, 2016; Accepted: September 10, 2016

The effect of the partial substitution of Al for Ag in the glass forming ability (GFA) of the $Zr_{57.52}Co_{21.24}Al_{21.24-x}Ag_x$ ($x = 8, 10, 12$, and 14 at. %) family alloy are reported and discussed. Cylindrical and conical ingots were obtained using the suction casting technique. It was found that the $Zr_{57.52}Co_{21.24}Al_{9.24}Ag_{12}$ alloy showed a glassy structure, with a critical glassy diameter, D_c , of 2 mm and $\Delta T_x = 41$ K. The bulk metallic glass $Zr_{57.52}Co_{21.24}Al_{9.24}Ag_{12}$ alloy was examined using scanning electron microscopy, differential thermal analysis and mechanical compression test. This alloy showed a Young's modulus (E) of 76.4 GPa and yield strength (σ_y) of 1.58 GPa. The Glass Forming Ability of the $Zr_{57.52}Co_{21.24}Al_{9.24}Ag_{12}$ was explained in terms of the topological model of dense packed clusters and kinetic fragility index of the alloy.

Keywords: *Metallic glass, fragility index, packing efficiency, glass formation*

1. Introduction

The Zr-based bulk metallic glass alloys are characterized by high strength (1.5 GPa), high elastic strain limit (~2%) and relatively low Young's modulus (50 - 100 GPa) and excellent corrosion resistance. Therefore, these alloys have already found some potential applications in the industry¹. On other hand, the high corrosion resistance and low in-vitro cytotoxicity of Zr-Co-Al-Ag bulk metallic glasses (BMGs) suggest an initial biocompatibility for biomedical applications².

Zhang et al. reported the partial substitution Co for Ag in $Zr_{53}Co_{23.5-x}Al_{23.5}Ag_x$ ($x = 0, 1, 3, 5, 7, 9$ at %) using copper mold casting technique³. They identified the best glass forming ability (GFA) at $x = 5$ ($Zr_{53}Co_{18.5}Al_{23.5}Ag_5$), which a critical diameter (D_c) of 10 mm, but with further increments of Ag content, D_c decreased down to 5 mm, for $x = 7$ and $x = 9$. This alloy demonstrated the sensitivity of small changes in chemical composition on the glass forming ability.

In order to explain the glass forming ability in metallic glasses, criteria based on transformation temperatures have been proposed, such as $\Delta T_x = T_x - T_g$ parameter, among many others⁴⁻⁶. However, such parameters can only be calculated after the glassy phase has been experimentally obtained. Also, theoretical formulations have been proposed to explain and calculate the glass formation in alloy systems, such as the topological model of densely packed clusters⁷⁻⁹. This model has claimed to help designing the chemical compositions of any alloy with high GFA. The topological model is based on a sphere-packing scheme (solute-centered clusters occupying an fcc cluster unit cell) and includes the calculation of three-

dimensional coordination number N^T , which is obtained for a radius ratio, R , for maximum packing efficiency⁷. Base on the model the packing efficiency can be calculated from the chemical composition and cluster unit cell length^{8,9}.

On the other hand, Angell has introduced the concept of fragility, which is defined as the increasing rate of the viscosity of a supercooled liquid at the glass transition temperature, during the cooling process. From this concept, the term "kinetic fragility, m ", was proposed as a good indicator of metallic glass formation. The magnitude of m , is defined in terms of the shear viscosity^{10,11}:

$$m = \left. \frac{\partial \log \eta(T)}{\partial \log (T_g/T)} \right|_{T=T_g} \quad (1)$$

Therefore, m is an index that shows how fast the viscosity increases while approaching the structural arrest at T_g , the temperature at which the viscosity $\eta = 10^{12}$ Pa s⁵. The kinetic fragility index, m , was used as a glass forming parameter, being calculated as follows¹²:

$$m = 12 \left(\frac{K}{G} + 0.67 \right) \quad (2)$$

where, m is the kinetic fragility index, K is the bulk modulus (GPa) and G is the shear modulus (GPa).

Form the resulting value of m , the glass-forming liquids can be classified into strong and fragile liquids. The upper and lower limits of parameter are theoretically estimated between 16 for 'strong' systems with high glass forming ability and 200 for 'fragile' systems with low glass forming ability¹².

* e-mail: borjas.ce@gmail.com

The topological model of densely packed clusters and the kinetic fragility index, m , have been used in the design of BMG in quaternary alloys systems¹³. Based on these models, several Zr-Co-Al-Ag alloys were calculated, and the effect of the partial substitution of Al for Ag in the glass forming ability was experimentally investigated. In this work, the GFA is explained in terms of the topological model of densely packed clusters, kinetic fragility index and thermal parameters. In addition, the mechanical properties for the $Zr_{57.52}Co_{21.24}Al_{9.24}Ag_{12}$ glassy alloy are presented.

2. Theoretical calculations and experimental procedure

2.1 Theoretical chemical compositions calculations

Chemical compositions of the Zr-Co-Al-Ag system were calculated using the topological model of densely packed clusters⁷⁻⁹. First, the calculations of atomic radii ratios, $R = r_i/r_\Omega$, between the solute atoms, r_i ($i = \alpha, \beta$ and γ) and solvent atoms, r_Ω , were carried out. Depending on the R value, the number of coordination, N^T , was calculated using equations (3-5)⁷.

$$N^T = \frac{4\pi}{6 \arccos\left(\sin\left(\frac{\pi}{3}\right)\left[1 - \frac{1}{(R+1)^2}\right]^{\frac{1}{2}}\right) - \pi} \quad 0.225 \leq R < 0.414 \quad (3)$$

$$N^T = \frac{4\pi}{8 \arccos\left(\sin\left(\frac{\pi}{4}\right)\left[1 - \frac{1}{(R+1)^2}\right]^{\frac{1}{2}}\right) - 2\pi} \quad 0.414 \leq R < 0.902 \quad (4)$$

$$N^T = \frac{4\pi}{10 \arccos\left(\sin\left(\frac{\pi}{5}\right)\left[1 - \frac{1}{(R+1)^2}\right]^{\frac{1}{2}}\right) - 3\pi} \quad 0.902 \leq R \quad (5)$$

For the quaternary system, it was considered that each atomic specie was accommodated in its corresponding place of the fcc cell clusters. Therefore, the number of solvent atoms, N_Ω , was calculated as follows⁹:

$$N_\Omega = \frac{N_\alpha}{1 + \frac{12}{N_\alpha}} \quad (6)$$

where, N_α is the number of coordination calculated with equation (4).

The chemical composition was obtained with the total number of atoms resulting from the sum of $N_\Omega + 1\alpha + 1\beta + 2\gamma$, because in the fcc packing, there is 1 β site and 2 γ sites for each α site⁸. The α and β concentrations are the same

and it is possible to obtain various chemical compositions considering different positions of the solute atoms in the cluster cell.

2.2. Efficiency packing calculations

In order to determine the cell cluster volume, V_{cell} , for each calculated composition, equations (7-9) were used⁹. The $d_{<100>}$, $d_{<110>}$ y $d_{<111>}$ distances were compared and the distance of greater magnitude, Λ_o , was used to calculate the cell cluster volume, Λ_o^3 .

$$d_{<100>} = 2r_\Omega \left[\sqrt{(R_\alpha + 1)^2 - \frac{4}{3}} + \sqrt{(R_\beta + 1)^2 - \frac{4}{3}} \right] \quad (7)$$

$$d_{<110>} = 4r_\Omega \left[\sqrt{(R_\alpha + 1)^2 - \frac{4}{3}} \right] \quad (8)$$

$$d_{<111>} = 2r_\Omega \left[\frac{\sqrt{(R_\alpha + 1)^2 - \frac{4}{3}} + \sqrt{(R_\beta + 1)^2 - \frac{4}{3}}}{2\sqrt{(R_\gamma + 1)^2 - \frac{4}{3}}} \right] \quad (9)$$

where, R_α , R_β y R_γ are atomic radii ratios of r_i/r_Ω , $i = \alpha, \beta$ and γ .

The packaging efficiency value, EP, is directly proportional to the glass forming ability. EP is calculated as follows:

$$EP = \frac{V_{at}}{V_{cell}} \quad (10)$$

where, V_{at} is the volume of the atoms in the fcc cluster cell and V_{cell} is the volume occupied by the cell clusters.

2.3. Fragility index calculation

The fragility index for the calculated composition was obtained with equation (2). The values of bulk modulus, K (GPa) and shear modulus, G , (GPa) were determined with the "rule of mixtures"¹⁴ and finally, the calculated compositions were classified according to the resulted m value obtained from the equation (2).

2.4. Experimental procedure

Alloy ingots with nominal composition of $Zr_{57.52}Co_{21.24}Al_{21.24-x}Ag_x$ ($x = 8, 10, 12$ and 14 at %) were prepared from elemental metals of pure Zr, Co, Al, Ag (purity > 99.8) by arc – melting, under a Ti gettered Ar atmosphere. The ingots were remelted five times to ensure chemical homogeneity. The alloy compositions represent the nominal values since the weight losses in melting were negligible (<0.1 %). Conical alloy ingots of length 30 mm, minimum diameter of 1 mm and maximum diameter of 8 mm, were produced by copper mould suction-casting within the argon arc furnace. Similarly, ingots of 2 mm in diameter and 37 mm length were produced. The conical

ingots were cut crosswise in 2 - 3 mm of diameter and verified by X-ray diffractometry by means of a Siemens D5000 diffractometer using Cu K α radiation to determine the critical glassy diameter, D_c . Cylindrical samples were used for compression test, being performed at a strain rate of 0.016 s^{-1} , using a Zwick Roell testing machine at room temperature. Scanning electron microscopy (SEM) JEOL JMS 600 equipped with an energy dispersive X-ray spectrometer EDX was used for elemental mapping (chemical homogeneity) and microstructural analysis; thermal behaviour was investigated by using a differential scanning calorimeter TA instruments SDT-Q600 in a flow of argon atmosphere at a heating rate of 0.67 K s^{-1} .

3. Results and discussion

3.1. Glass formation

Figure 1 Shows the conical and cylindrical ingots obtained by the suction casting technique. The suction casting technique is normally used in order to obtain a glassy phase and has been used by other scientists^{15, 16}. The ingots showed metallic luster, which indicates that the preparation process did prevent the oxidation of the alloys. The $\text{Zr}_{57.52}\text{Co}_{21.24}\text{Al}_{9.24}\text{Ag}_{12}$ cylindrical bar was useful for mechanical testing and the conical ingots were useful for determining the critical glassy diameter.

Figure 2 displays the X ray diffraction patterns of alloys with 3 mm section. The patterns of XRD shows the presence of sharp peaks in $2\theta \sim 30^\circ - 50^\circ$, which indicates that the alloys analysed have a partly crystalline structure.

Figure 3 shows the XRD patterns of cast alloys with 2 mm cross-section. The $\text{Zr}_{57.52}\text{Co}_{21.24}\text{Al}_{9.24}\text{Ag}_{12}$ alloy shows a diffuse diffraction pattern localized between $2\theta \sim 35^\circ - 50^\circ$ without a detectable sharp Bragg peak. Therefore, this alloy can be considered as BMG with a critical diameter, D_c , of 2 mm. These showed that the substitution of Al for Ag increased the glass formation for a silver content of 12 at%. However, the rest of the alloys had partly crystalline structure.

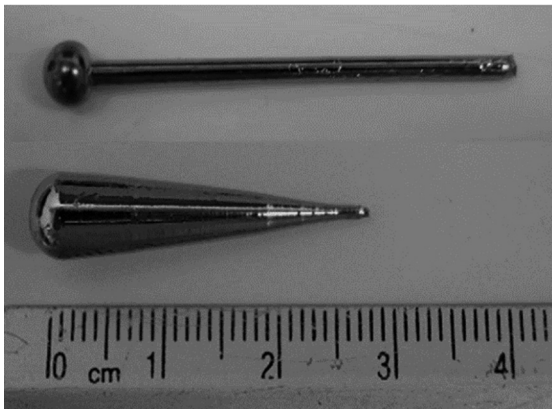


Figure 1: Conical and cylindrical ingots obtained for suction casting.

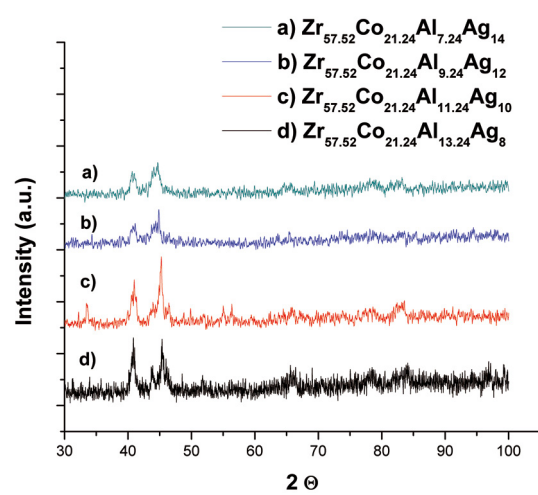


Figure 2: XRD patterns for Zr-Co-Al-Ag alloys of 3 mm cross-section.

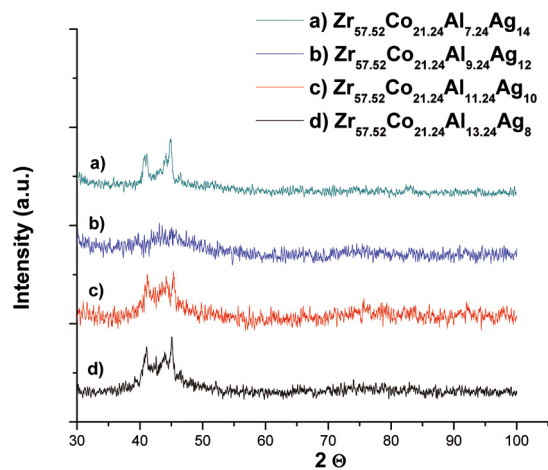


Figure 3: XRD patterns for Zr-Co-Al-Ag alloys of 2 mm cross-section.

Figure 4 shows an elemental EDS mapping taken from the scanning electron microscope. The EDX analysis indicates the chemical homogeneity in the $\text{Zr}_{57.52}\text{Co}_{21.24}\text{Al}_{9.24}\text{Ag}_{12}$ lower zone ingot (2 mm diameter). From this figure, it is evident that no atomic segregation was found, the mapping shows a homogeneous atomic distribution in the as cast bulk metallic glass sample.

Table 1 shows the packing efficiency values, PE, for the calculated compositions with the topologic model reported in references 7-9. The different compositions resulted in the position interchange of the solute atoms of the cell clusters. Table 1, also includes the estimated values corresponding to the fragility index. The $\text{Zr}_{57.52}\text{Al}_{10.62}\text{Ag}_{10.62}\text{Co}_{21.24}$ calculated composition showed the highest PE value (45.35%) and a fragility index close to 16. Thus, $\text{Zr}_{57.52}\text{Al}_{10.62}\text{Ag}_{10.62}\text{Co}_{21.24}$ alloy can be classified into the category of strong liquids, according to Angell's classification^{10, 11}.

The $\text{Zr}_{57.52}\text{Ag}_{10.62}\text{Al}_{10.62}\text{Co}_{21.24}$ and $\text{Zr}_{57.52}\text{Ag}_{10.62}\text{Co}_{10.62}\text{Al}_{21.24}$ calculated compositions have the same fragility index

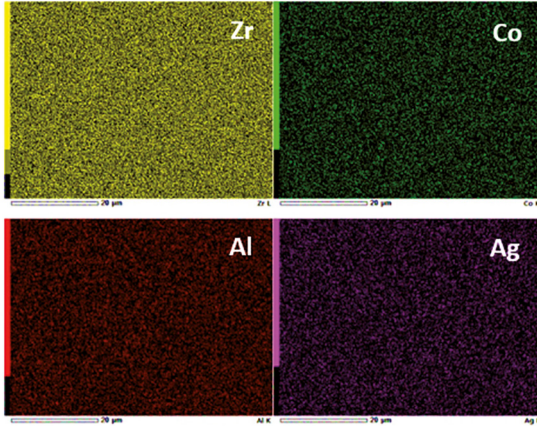


Figure 4: EDX Mapping of $Zr_{57.52}Co_{21.24}Al_{9.24}Ag_{12}$ BMG in 2 mm cross-section.

Table 1: Compositions, packaging efficiency and fragility index in Zr-Co-Al-Ag system

Chemical composition	Efficiency Packing EP %	Fragility index m
$Zr_{57.52}Ag_{10.62}Al_{10.62}Co_{21.24}$	45.37	40.1
$Zr_{57.19}Al_{10.70}Ag_{10.70}Co_{21.41}$	44.96	41.1
$Zr_{57.52}Ag_{10.62}Co_{10.62}Al_{21.24}$	43.37	40.1
$Zr_{57.19}Al_{10.70}Co_{10.70}Ag_{21.41}$	42.86	41.6
$Zr_{52.38}Co_{11.91}Ag_{11.91}Al_{23.81}$	37.9	41.1
$Zr_{52.38}Co_{11.91}Al_{11.91}Ag_{23.81}$	37.8	41.6

value (40.1). However, for the $Zr_{57.52}Ag_{10.62}Al_{10.62}Co_{21.24}$ the EP value was higher (45.37 EP %). This indicates that the $Zr_{57.52}Ag_{10.62}Al_{10.62}Co_{21.24}$ could have a higher GFA. On other hand, the $Zr_{57.52}Ag_{10.62}Al_{10.62}Co_{21.24}$ and $Zr_{57.19}Al_{10.70}Ag_{10.70}Co_{21.41}$ calculated compositions are practically the same, but $Zr_{57.52}Ag_{10.62}Al_{10.62}Co_{21.24}$ had slightly higher GFA, according to the EP % and m parameters.

The fragility index for $Zr_{41}Ti_{14}Cu_{12.5}Ni_{10}Be_{22.5}$ (50), $Zr_{35}Ti_{30}Cu_{8.25}Be_{26.75}$ (60) and $Zr_{46.75}Ti_{8.25}Cu_{7.5}Ni_{10}Be_{27.5}$ (44) glasses was higher than Zr -Ag-Al-Co (40.1) calculated compositions. This indicates that the investigated compositions have higher GFA. The values of m normally range from 20 to 70 for the BMGs¹⁴.

The $Zr_{57.52}Ag_{10.62}Al_{10.62}Co_{21.24}$ calculated composition is closed to $Zr_{57.52}Co_{21.24}Al_{9.24}Ag_{12}$ experimentally obtained. In addition, the similarity in concentration of Zr and Co between the $Zr_{57.52}Ag_{10.62}Al_{10.62}Co_{21.24}$ calculated composition respect to $Zr_{56}Al_{16}Co_{28}$ reported ternary system with a near-eutectic composition is significant³.

Figure 5a shows the thermal analysis of the $Zr_{57.52}Co_{21.24}Al_{9.24}Ag_{12}$ glassy alloy composition. This indicates the transformation temperatures, such as glass transition temperature, T_g , crystallization temperature, T_x , melting temperature, T_m and liquidus temperature, T_l . The

crystallization peaks, P_1 and P_2 are clearly displayed. The first crystallization peak is evident in the derivative curve of heat flow, as shown in Figure 5b.

Table 2 shows the values of transformation temperatures and the GFA parameters. The ΔT_x and D_c values in $Zr_{57.52}Co_{21.24}Al_{9.24}Ag_{12}$ are 41 K and 2 mm, respectively. It has lower GFA regarding to reported glasses in the same system, such as $Zr_{53}Co_{23.5-x}Al_{23.5}Ag_x$ ($x = 0, 1, 3, 5, 7, 9$) family alloys, whose values are between $\Delta T_x = 52$ -69 K and $D_c = 3$ -10 mm³. However, the $Zr_{57.52}Co_{21.24}Al_{9.24}Ag_{12}$ GFA is very similar to $Zr_{67}Co_{18}Al_7Pd_3Nb_3$ BMG with $\Delta T_x = 37$ K¹⁷.

Figure 6 shows the microstructural evolution depending on the conical diameter ingot of the $Zr_{57.52}Co_{21.24}Al_{9.24}Ag_{12}$ alloys. It is also possible to observe qualitatively the suppression of crystalline phases with decreasing longitudinal section due to increase in the cooling rate. The advantage of casting in a conical shaped mould is that the cooling rate varies for top bottom, i.e. the cooling rate is much faster at thinner sections that thicker ones, therefore, the study of the critical glassy diameter is more precise. According to Figueroa, the cooling rate for glass formation in sections of 2 mm is between 770 - 885 ks⁻¹, for an Al-Cu alloys, obtained by means of measuring the secondary dendrite arm spacing (γ_2)¹⁵. It is important to notice that although the alloys investigated in this work are different, the cooling rate reported for the Al based alloy could give a good approximation of the actual system. In other words, the cooling rate is a function of both the alloy composition and casting parameters used; therefore, these rates give only an indication of the cooling rate attainable when casting BMG's.

3.2 Mechanical properties

Figure 7 shows a compression stress-strain curve of the $Zr_{57.52}Co_{21.24}Al_{9.24}Ag_{12}$ bulk metallic glass. The yield stress is similar to those reported for Zr-based glassy alloys (1.58 GPa)¹. The compressive modulus and the elastic deformation values were 76.4 GPa and 2 %, respectively.

The Young's modulus (80.2 GPa) was calculated by the "rule of mixtures"¹⁴, which is closed to the experimental value (76.4 GPa). Both, the yield stress, σ_y , and the Young's modulus values were quite similar to those reported for Zr-based multicomponent glassy alloys¹⁴: $Zr_{65}Cu_{15}Ni_{10}Al_{10}$ (1.4, 80), $Zr_{59}Ta_3Cu_{18}Ni_8Al_{10}$ (1.8, 96), $Zr_{41.2}Ti_{13.8}Cu_{12.5}Ni_{10}Be_{22.5}$ (1.7, 97) -values given in GPa-.

4. Conclusions

It was possible to obtain the $Zr_{57.52}Co_{21.24}Al_{9.24}Ag_{12}$ alloy with glassy structure with the substitution of Al for Ag in $Zr_{57.52}Co_{21.24}Al_{21.24-x}Ag_x$ ($x = 8, 10, 12$, and 14 at. %) family alloy. The critical glassy diameter for the vitrified alloy was

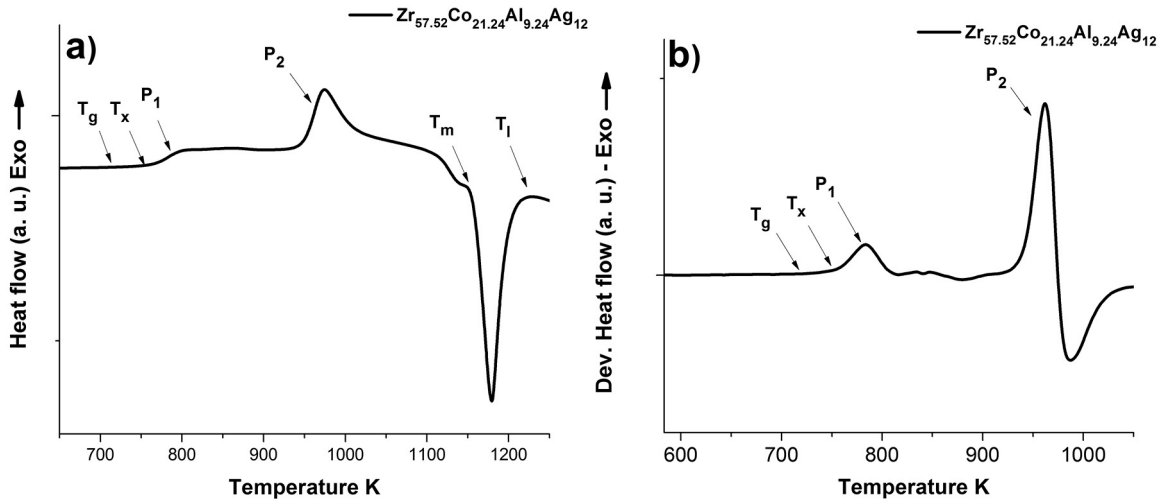


Figure 5: Thermal analysis of Zr-Co-Al-Ag BMG, with a $D_c = 2$ mm, at heating rate of 0.67 K s^{-1} .

Table 2: Transformation temperatures and GFA parameters of the $\text{Zr}_{57.52}\text{Co}_{21.24}\text{Al}_{9.24}\text{Ag}_{12}$ BMG, with a $D_c = 2$ mm.

Transformation temperatures				GFA parameters	
T_g (K)	T_x (K)	T_m (K)	T_l (K)	ΔT_x (K)	D_c (mm)
710	751	1146	1197	41	2

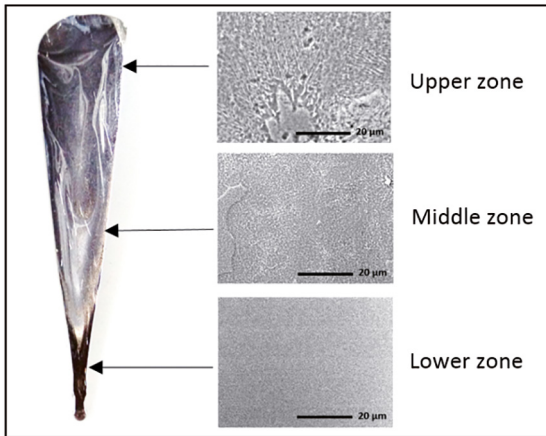


Figure 6: Conical ingot microstructures observed by scanning electron microscopy of the $\text{Zr}_{57.52}\text{Co}_{21.24}\text{Al}_{9.24}\text{Ag}_{12}$ BMG.

found to be 2 mm and $\Delta T_x = 41$ K. The criterion of compact packing model was useful to determine the chemical composition range in order to obtain a BMG. The $\text{Zr}_{57.52}\text{Co}_{21.24}\text{Al}_{10.62}\text{Ag}_{10.62}$ composition, theoretically calculated with this model presented a high packing efficiency, which can be found between the experimentally obtained partly crystalline $\text{Zr}_{57.52}\text{Co}_{21.24}\text{Al}_{11.24}\text{Ag}_{10}$ alloy and the fully $\text{Zr}_{57.52}\text{Co}_{21.24}\text{Al}_{9.24}\text{Ag}_{12}$ vitreous alloy. In this work, the usage of the compact packing criterion and fragility index resulted rather useful in designing the chemical composition for obtaining a bulk metallic glass.

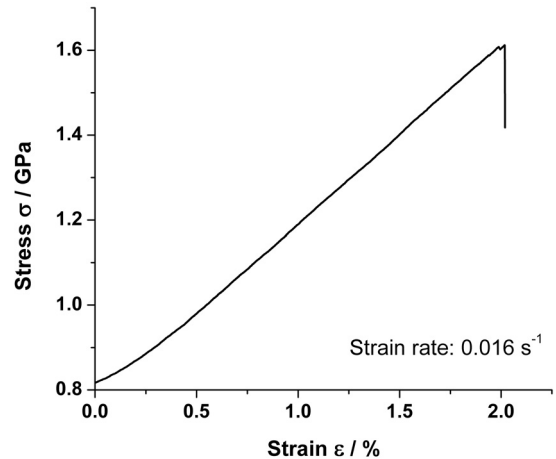


Figure 7: Stress-strain curve of the $\text{Zr}_{57.52}\text{Co}_{21.24}\text{Al}_{9.24}\text{Ag}_{12}$ bulk metallic glass ($D_c = 2$ mm).

5. Acknowledgment

The authors would like to acknowledge the financial support from SEP CONACYT through the 178289 grant. C. Soto thanks CONACYT for the 232312 scholarship grant. A. Tejada-Cruz, C. Flores, A. Lopez V. and O. Novelo are also acknowledged for their technical support.

6. References

1. Suryanarayana C, Inoue A. *Bulk metallic glasses*. Boca Raton: CRC Press Taylor & Francis Group; 2012.
2. Hua N, Huang L, Wang J, Cao Y, He W, Pang S, et al. Corrosion behavior and *in vitro* biocompatibility of Zr-Al-Co-Ag bulk metallic glasses: An experimental case study. *Journal of Non-Crystalline Solids*. 2012;358(12-13):1599-1604.

3. Zhang C, Li N, Pan J, Guo SF, Zhang M, Liu L. Enhancement of glass-forming ability and bio-corrosion resistance of Zr–Co–Al bulk metallic glasses by the addition of Ag. *Journal of Alloys and Compounds*. 2010;504(Supp 1):S163-S167.
4. Inoue A. High Strength Bulk Amorphous Alloys with Low Critical Cooling Rates (Overview). *Materials Transactions*. 1995;36(7):866-875.
5. Turnbull D. Under what conditions can a glass be formed? *Contemporary Physics*. 1969;10(5):473-488.
6. Kim JH, Park JS, Lim HK, Kim WT, Kim DH. Heating and cooling rate dependence of the parameters representing the glass forming ability in bulk metallic glasses. *Journal of Non-Crystalline Solids*. 2005; 351(16-17):1433-1440.
7. Miracle DB, Sanders WS, Senkov ON. The influence of efficient atomic packing on the constitution of metallic glasses. *Philosophical Magazine*. 2003;83(20):2409-2428.
8. Miracle DB. The efficient cluster packing model – An atomic structural model for metallic glasses. *Acta Materialia*. 2006;54(16):4317-4336.
9. Miracle DB. A structural model for metallic glasses. *Nature Materials*. 2004;3:697-702.
10. Angell CA. Formation of glasses from liquids and biopolymers. *Science*. 1995; 267(5206): 1924-1935.
11. Böhmer R, Ngai KL, Angell CA, Plazek DJ. Nonexponential relaxations in strong and fragile glass formers. *The Journal of Chemical Physics*. 1993; 99(5): 4201-4209. <http://dx.doi.org/10.1063/1.466117>
12. Park ES, Na JH, Kim DH. Correlation between fragility and glass-forming ability/plasticity in metallic glass forming alloys. *Applied Physics Letters*. 2007;91:031907.
13. Borja Soto CE, Figueroa Vargas IA, Fonseca Velázquez JR, Lara Rodríguez GA, Verduzco Martínez JA. Composition, elastic property and packing efficiency predictions for bulk metallic glasses in binary, ternary and quaternary systems. *Materials Research*. 2016;19(2):285-294. <http://dx.doi.org/10.1590/1980-5373-MR-2015-0537>.
14. Wang WH. The elastic properties, elastic models and elastic perspectives of metallic glasses. *Progress in Materials Science*. 2012; 57 487-656.
15. Figueroa IA, Carroll PA, Davies HA, Jones H, Todd I. Preparation of Cu-based bulk metallic glasses by suction casting. In: *Proceedings of the Fifth Decennial International Conference on Solidification Processing*; 2007 July 23-25; Sheffield, UK. p. 479-482.
16. Liu GR. A step-by-step method of rule-of-mixture of fiber- and particle-reinforced composite materials. *Composite Structures*. 1997;40(3-4):313-322.
17. Zhu S, Guoqiang X, Qin F, Wang X, Inoue A. Ni- and Be-free Zr-based bulk metallic glasses with high glass-forming ability and unusual plasticity. *Journal of the Mechanical Behavior of Biomedical Materials*. 2012;13:166-173.